

Influence of Active Vehicle Suspension to Maintain Transverse Stability in Bends

Hristo Uzunov¹, Stanimir Karapetkov¹, Lubomir Dimitrov²,
Silvia Dechkova¹✉ and Vasil Uzunov¹

¹ Technical University of Sofia, Faculty and College – Sliven, Bulgaria
si_yana@abv.bg

² Technical University of Sofia, Kliment Ohridski Blvd., Sofia 1000, Bulgaria

Abstract. Active control systems of today's cars have been used over a vast domain of applications, as they seem to represent a complex compromise between car handling, stability and ride comfort. Finding a balance between these three components is of paramount importance to stability, a well-known prerequisite, directly proportional, for road safety. Active suspension means active control of certain parameters of vehicle suspension and their changes over time in their equilibrium state. The aim is to maintain vehicle stability going round bends. Setting a tolerance for these parameters results in a compromise in ride quality of vehicle carbody. This is usually accomplished by changing the elasticity of the springs in suspension and increasing their elastic constant to hardening. Thus, a minimum tolerance in the rotation of the carbody around the transverse and longitudinal axes can be guaranteed, respectively a reduction of the centrifugal inertial forces as a function of the rotation defined. To solve this problem a dynamic study of a car model is needed, taking into account elasticity of spring suspension and wheel suspensions, dampers and tyre damping as well as tire-road friction forces. An indicator of this is the variable friction coefficient as a function of the velocity of the contact point.

Keywords: Automobile, Active suspension, Dynamic model, Failure, Matlab.

1 Introduction

Vehicle motion planning, generally, is spatial, defined by six generalized coordinates. For this purpose, coordinates of vehicle centers of mass x_C, y_C, z_C , are used in a fixed coordinate system, as well as three Euler angles φ, ψ, θ . A fixed coordinate system $Oxyz$ and a mobile one $Cx'y'z'$, constantly fixed to the vehicle, have been chosen. Euler's dependences are also used to transform the mobile coordinate system to the fixed one. [1–4].

2

2 Dynamic Model of Active Car Suspension

Macro simulation of vehicle motion in case of loss of lateral stability is observed in an arbitrarily accepted absolute coordinate system $OXYZ$ [5–10]. To study the car motion, it has been assumed that its own coordinate system $Cx'y'z'$ is movable and permanently connected to the vehicle center of mass C (Fig. 1a). In addition, a permanently connected $Cxyz$ coordinate system is attached to it, parallel to the absolute and translationally movable one.

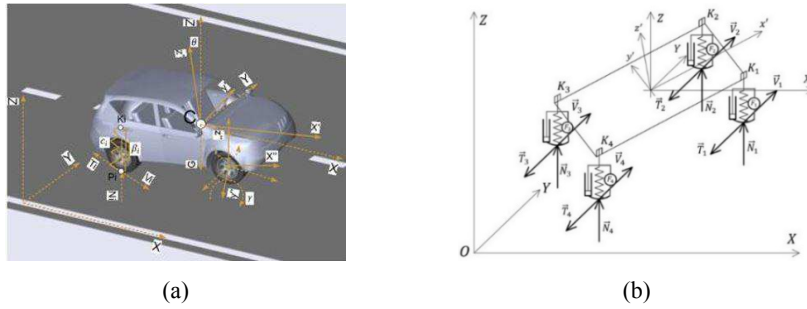


Fig. 1. (a) Spatial dynamic model of an automobile with elastic suspension and (b) Model of the forces acting on a car in its spatial motion, taking into account the elasticity of tires (suspension).

Coordinates of the vehicle center of mass C x_c, y_c, z_c in the fixed coordinate system are selected for generalized coordinates of the car motion.

Rotational motion of the car is expressed by the Euler transformations and corresponding angles, namely ψ, θ and φ . The precession angle of ψ , taking into account the rotation around the axis Cz ; respectively, the angular velocity of $\dot{\psi}$ is obtained; the angle θ of nutation, taking into account the rotation with respect to the axis $C\rho$, the intersection of the planes Oxy and $Cx'y'$.

Therefore, the force of gravity \vec{G} will lie on the axis Oz . The spatial arrangement model of the car is a plane located on four elastic supports, which are marked by $K_i (i = 1 \div 4)$ (Fig. 1b).

$\vec{F}_i (i = 1 \div 4)$ is elastic force generated by the elasticity of tires and springs; $\vec{N}_i (i = 1 \div 4)$ is normal reaction at the contact point of automobile tires, corresponding to elastic force; $\vec{V}_i (i = 1 \div 4)$ is velocity of the contact point P_i in the plane of the road Oxy ; $\vec{T}_i (i = 1 \div 4)$ is friction force at the contact points that lies in the plane of the road Oxy ; $\vec{R}_i (i = 1 \div 4)$ is resistance force generated by damping elements in suspension; $c_i, \frac{N}{m} (i = 1 \div 4)$ elasticity of suspension, taking into account both coefficient of elasticity of tires and suspension; $b_i, \frac{N \cdot s}{m} (i = 1 \div 4)$ coefficient of linear resistance.

The car motion according to the studies of kinetic energy and generalized forces is defined by six differential equations with six generalized coordinates. These equations are valid if the friction force is in accordance with Coulomb's law and the wheels slide on the ground without rolling. According to (5), the wheels keep a continuous contact with the road.

3

Generalized forces and moments in the right-hand sides of the differential equations (1) are determined by assuming that the absolute coordinate system has a vertical axis of Oz [11–14]:

$$\begin{aligned} m \cdot \ddot{x} &= [\sum_{i=1}^4 F_{xi}] \\ m \cdot \ddot{y} &= [\sum_{i=1}^4 F_{yi}] \\ m \cdot \ddot{z} &= [-G + \sum_{i=1}^4 N_i - \sum_{i=1}^4 R_i] \end{aligned} \quad (1)$$

$$\begin{aligned} & a_{11} \cdot \ddot{\varphi} + a_{12} \cdot \ddot{\psi} + a_{13} \cdot \ddot{\theta} = \\ = & \left\{ \begin{aligned} & \sum_{i=1}^4 N_i \cdot \delta_{\varphi i} + \sum_{i=1}^4 (F_{xi} \cdot f_{\varphi xi} + F_{yi} \cdot f_{\varphi yi}) - \sum_{i=1}^4 R_i \cdot \delta_{\varphi i} - \\ & -b_{11} \cdot \dot{\varphi}^2 - b_{12} \cdot \dot{\psi}^2 - b_{13} \cdot \dot{\theta}^2 - c_{11} \cdot \dot{\varphi} \cdot \dot{\psi} - c_{12} \cdot \dot{\varphi} \cdot \dot{\theta} - c_{13} \cdot \dot{\psi} \cdot \dot{\theta} \end{aligned} \right\} \end{aligned} \quad (2)$$

$$\begin{aligned} & a_{21} \cdot \ddot{\varphi} + a_{22} \cdot \ddot{\psi} + a_{23} \cdot \ddot{\theta} = \\ = & \left\{ \begin{aligned} & \sum_{i=1}^4 (F_{xi} \cdot f_{\psi xi} + F_{yi} \cdot f_{\psi yi}) - b_{21} \cdot \dot{\varphi}^2 - b_{22} \cdot \dot{\psi}^2 - b_{23} \cdot \dot{\theta}^2 - \\ & -c_{21} \cdot \dot{\varphi} \cdot \dot{\psi} - c_{22} \cdot \dot{\varphi} \cdot \dot{\theta} - c_{23} \cdot \dot{\psi} \cdot \dot{\theta} \end{aligned} \right\} \end{aligned} \quad (3)$$

$$\begin{aligned} & a_{31} \cdot \ddot{\varphi} + a_{32} \cdot \ddot{\psi} + a_{33} \cdot \ddot{\theta} = \\ = & \left\{ \begin{aligned} & \sum_{i=1}^4 N_i \cdot \delta_{\theta i} + \sum_{i=1}^4 (F_{xi} \cdot f_{\theta xi} + F_{yi} \cdot f_{\theta yi}) - \sum_{i=1}^4 R_i \cdot \delta_{\theta i} - \\ & -b_{31} \cdot \dot{\varphi}^2 - b_{32} \cdot \dot{\psi}^2 - b_{33} \cdot \dot{\theta}^2 - c_{31} \cdot \dot{\varphi} \cdot \dot{\psi} - c_{32} \cdot \dot{\varphi} \cdot \dot{\theta} - c_{33} \cdot \dot{\psi} \cdot \dot{\theta} \end{aligned} \right\} \end{aligned} \quad (4)$$

$$\begin{aligned} a_{11} &= J_{z'z'} \\ a_{12} &= -J_{z'z'} \cdot \cos\theta - J_{z'x'} \cdot \sin\varphi \cdot \sin\theta - J_{y'z'} \cdot \cos\varphi \cdot \sin\theta \\ a_{13} &= -J_{z'x'} \cdot \cos\varphi + J_{y'z'} \cdot \sin\varphi \end{aligned} \quad (5)$$

$$\begin{aligned} b_{11} &= 0 \\ b_{12} &= \left(-\frac{1}{2} \cdot \sin 2\varphi \cdot \sin^2\theta \cdot (J_{x'x'} + J_{y'y'}) + J_{x'y'} \cdot \cos 2\varphi \cdot \sin^2\theta + \right. \\ & \left. + \frac{1}{2} \cdot \sin 2\theta \cdot (J_{z'x'} \cdot \cos\varphi - J_{y'z'} \cdot \sin\varphi) \right) \\ b_{13} &= \left(\frac{1}{2} \cdot (J_{x'x'} - J_{y'y'}) \cdot \sin 2\varphi - J_{x'y'} \cdot \cos 2\varphi \right) \end{aligned} \quad (6)$$

$$\begin{aligned} c_{11} &= 0; \quad c_{12} = 0 \\ c_{13} &= \left(\cos 2\varphi \sin\theta (J_{x'x'} + J_{y'y'}) - J_{z'z'} \cdot \sin\theta - 2 \left(\begin{aligned} & J_{x'y'} \cdot \sin 2\varphi \sin\theta + \\ & + J_{z'x'} \cdot \sin\varphi \cos\theta + \\ & + J_{y'z'} \cdot \cos\varphi \cos\theta \end{aligned} \right) \right) \end{aligned} \quad (7)$$

$$\begin{aligned} a_{21} &= (J_{z'z'} \cdot \cos\theta - J_{z'x'} \cdot \sin\varphi \cdot \sin\theta - J_{y'z'} \cdot \cos\varphi \cdot \sin\theta) \\ a_{22} &= \left(\begin{aligned} & J_{x'x'} \cdot \sin^2\varphi \cdot \sin^2\theta + J_{y'y'} \cdot \cos^2\varphi \cdot \sin^2\theta + \\ & + J_{z'z'} \cdot \cos^2\theta - J_{x'y'} \cdot \sin 2\varphi \cdot \sin^2\theta \\ & - J_{z'x'} \cdot \sin\varphi \cdot \sin 2\theta - J_{y'z'} \cdot \cos\varphi \cdot \sin 2\theta \end{aligned} \right) \\ a_{23} &= \left(\begin{aligned} & 0,5 \cdot J_{x'x'} \cdot \sin 2\varphi \cdot \sin\theta - \frac{1}{2} \cdot J_{y'y'} \cdot \sin 2\varphi \cdot \sin\theta - \\ & - J_{x'y'} \cdot \cos 2\varphi \cdot \sin\theta - J_{z'x'} \cdot \cos\varphi \cdot \cos\theta + \\ & + J_{y'z'} \cdot \sin\varphi \cdot \cos\theta \end{aligned} \right) \end{aligned} \quad (8)$$

4

$$\begin{aligned}
b_{21} &= (-J_{z'x'} \cdot \cos\varphi + J_{y'z'} \cdot \sin\varphi) \cdot \sin\theta \\
b_{22} &= 0 \\
b_{23} &= \left(\begin{aligned} & \left(0,5 \cdot J_{x'x'} \cdot \sin 2\varphi - \frac{1}{2} \cdot J_{y'y'} \cdot \sin 2\varphi - J_{x'y'} \cdot \cos 2\varphi \right) \cos\theta + \\ & + (J_{z'x'} \cdot \cos\varphi - J_{y'z'} \cdot \sin\varphi) \cdot \sin\theta \end{aligned} \right) \quad (9)
\end{aligned}$$

$$\begin{aligned}
c_{21} &= \left(\begin{aligned} & (J_{x'x'} \cdot \sin 2\varphi - J_{y'y'} \cdot \sin 2\varphi - 2 \cdot J_{x'y'} \cdot \cos 2\varphi) \sin^2\theta - \\ & - (J_{z'x'} \cdot \cos\varphi - J_{y'z'} \cdot \sin\varphi) \cdot \sin 2\theta \end{aligned} \right) \\
c_{22} &= \left(\begin{aligned} & (J_{x'x'} \cdot \cos 2\varphi - J_{y'y'} \cdot \cos 2\varphi + 2 \cdot J_{x'y'} \cdot \sin 2\varphi) \sin\theta - \\ & - J_{z'z'} \cdot \sin\theta \end{aligned} \right) \quad (10) \\
c_{23} &= \left(\begin{aligned} & (J_{x'x'} \cdot \sin^2\varphi + J_{y'y'} \cdot \cos^2\varphi - J_{x'y'} \cdot \sin 2\varphi - J_{z'z'}) \sin 2\theta - \\ & - 2 \cdot (J_{z'x'} \cdot \sin\varphi + J_{y'z'} \cdot \cos\varphi) \cdot \cos 2\theta \end{aligned} \right)
\end{aligned}$$

$$\begin{aligned}
a_{31} &= J_{z'x'} \cdot \cos\varphi + J_{y'z'} \cdot \sin\varphi \\
a_{32} &= \left[\begin{aligned} & 0,5 \cdot (J_{x'x'} - J_{y'y'}) \cdot \sin 2\varphi \cdot \sin\theta - J_{x'y'} \cdot \cos 2\varphi \cdot \sin\theta - \\ & - J_{z'x'} \cdot \cos\varphi \cdot \cos\theta + J_{y'z'} \cdot \sin\varphi \cdot \cos\theta \end{aligned} \right] \quad (11) \\
a_{33} &= J_{x'x'} \cdot \cos^2\varphi + J_{y'y'} \cdot \sin^2\varphi + \frac{1}{2} \cdot J_{x'y'} \cdot \sin 2\varphi
\end{aligned}$$

$$\begin{aligned}
b_{31} &= J_{z'x'} \cdot \sin\varphi + J_{y'z'} \cdot \cos\varphi \\
b_{32} &= \left[\begin{aligned} & -[0,5(J_{x'x'} \sin^2\varphi + J_{y'y'} \cos^2\varphi + J_{z'z'} - J_{x'y'} \sin 2\varphi)] \sin 2\theta + \\ & + (J_{z'x'} \cdot \sin\varphi + J_{y'z'} \cdot \cos\varphi) \cdot \cos 2\theta \end{aligned} \right] \quad (12) \\
b_{33} &= 0
\end{aligned}$$

$$\begin{aligned}
c_{31} &= \left[\begin{aligned} & [(J_{x'x'} + J_{y'y'}) \cdot \cos 2\varphi + 2 \cdot J_{x'y'} \cdot \sin 2\varphi + J_{z'z'}] \cdot \sin\theta + \\ & + 2 \cdot (J_{z'x'} \cdot \sin\varphi + J_{y'z'} \cdot \cos\varphi) \cdot \cos\theta \end{aligned} \right] \quad (13) \\
c_{32} &= [(-J_{x'x'} + J_{y'y'}) \cdot \sin 2\varphi + 2 \cdot J_{x'y'} \cdot \cos 2\varphi] \\
c_{33} &= 0
\end{aligned}$$

We substitute the equations before $\delta_{\varphi i}$ and $\delta_{\theta i}$ using the notation:

$$\delta_{\varphi i} = [(\cos\varphi \cdot \sin\theta) \cdot x'_{ki} + (-\sin\varphi \cdot \sin\theta) \cdot y'_{ki}] \quad (14)$$

$$\delta_{\theta i} = [(\sin\varphi \cos\theta) \cdot x'_{ki} + (\cos\varphi \cos\theta) y'_{ki} + (-\sin\theta) \cdot z'_{ki}] \quad (15)$$

To facilitate notation, substitution has been done, which looks like as follows:

$$\begin{aligned}
f_{\varphi_{xi}} &= \left[\begin{aligned} & \left(\begin{aligned} & -\cos\psi \cdot \sin\varphi - \\ & -\sin\psi \cdot \cos\varphi \cdot \cos\theta \end{aligned} \right) \delta x'_{pi} + \\ & + \left(\begin{aligned} & -\cos\psi \cdot \cos\varphi + \\ & +\sin\psi \cdot \sin\varphi \cdot \cos\theta \end{aligned} \right) \delta y'_{pi} \end{aligned} \right]; \quad f_{\psi_{xi}} = \left[\begin{aligned} & \left(\begin{aligned} & -\sin\psi \cdot \cos\varphi - \\ & -\cos\psi \cdot \sin\varphi \cdot \cos\theta \end{aligned} \right) \delta x'_{ki} + \\ & + \left(\begin{aligned} & \sin\psi \cdot \sin\varphi - \\ & -\cos\psi \cdot \cos\varphi \cdot \cos\theta \end{aligned} \right) \delta y'_{ki} + \\ & + (-\cos\psi \cdot \sin\theta) \delta z'_{ki} \end{aligned} \right] \quad (16) \\
f_{\theta_{xi}} &= \left[\begin{aligned} & (\sin\theta \cdot \sin\psi \cdot \sin\varphi) \delta x'_{ki} + \\ & + (\sin\theta \cdot \sin\psi \cdot \cos\varphi) \delta y'_{ki} + \\ & + (-\cos\theta \cdot \sin\psi) \delta z'_{ki} \end{aligned} \right]
\end{aligned}$$

5

$$f_{\varphi_{yi}} = \begin{bmatrix} (-\sin\psi \cdot \sin\varphi + \cos\psi \cdot \sin\varphi \cdot \cos\theta) \delta x'_{ki} + \\ + (-\sin\psi \cdot \cos\varphi - \cos\psi \cdot \sin\varphi \cdot \cos\theta) \delta y'_{ki} \end{bmatrix}; \quad f_{\psi_{yi}} = \begin{bmatrix} (\cos\psi \cdot \cos\varphi - \sin\psi \cdot \sin\varphi \cdot \cos\theta) \delta x'_{ki} + \\ + (-\cos\psi \cdot \sin\varphi - \sin\psi \cdot \cos\varphi \cdot \cos\theta) \delta y'_{ki} + \\ + (\sin\psi \cdot \sin\theta) \delta z'_{ki} \end{bmatrix} \quad (17)$$

$$f_{\theta_y} = \begin{bmatrix} (-\cos\psi \cdot \sin\varphi \cdot \sin\theta) \delta x'_{ki} + \\ + (-\cos\psi \cdot \cos\varphi \cdot \sin\theta) \delta y'_{ki} + \\ + (-\cos\psi \cdot \sin\theta) \delta z'_{ki} \end{bmatrix}$$

The relative motion of the wheels, the differential(s) and the engine are characterized by a system of four differential equations derived by the Lagrangian method, which has the form of:

$$[L_y] \cdot [\ddot{\gamma}] = [M_{\gamma i}]; \quad M_{\gamma i} = \{F_{it} \cdot r_i + \text{sign}(\dot{\gamma}_i) \cdot [M_{di} - f_i \cdot N_i - M_{si}]\} \quad (18)$$

\vec{F}_{it} is tangential component of the tire-road friction force, the positive direction of which is taken backwards, in the more frequent cases of braking or loss of stiffness.

Where μ is friction coefficient depending on slipping speed on the contact spot; r_i – radius of the wheel; f_i – coefficient of rolling friction; N_i – normal reaction of the road on wheels; $[L_y]$ – a square matrix of coefficients in front the actual angular acceleration of the drive wheels, depending on the moment of inertia of the wheels and the engine; $\dot{\gamma}_i / i = 1 \div 4$ – wheel angular velocity; $[\ddot{\gamma}]$ – a matrix-column of the actual angular acceleration of the wheels, two or four of which are propulsive; M_{di}, M_{si} – corresponding engine and brake torque applied to each wheel.

Figure 2a shows the dynamic model of an active suspension system. Figure 2b shows the dynamic diagram of a driving or sliding wheel.

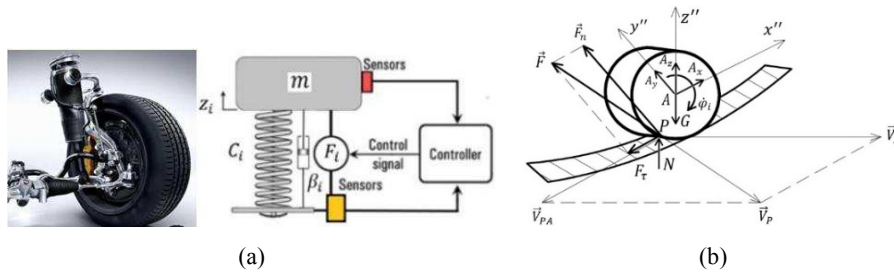


Fig. 2. (a) Dynamic model of an active suspension system and (b) Drive wheel diagram.

In the system solving the differential equations of motion, a module has been added for the analysis of the two angles of rotation $\varphi_{x'}$ and $\varphi_{y'}$, which are determined by the kinematic equations of Euler (16 and 17). They represent the rotation of the unsprung mass around its own coordinate system relative to a parallel moving coordinate system of the fixed coordinate system, invariably connected to its center of mass. Its change above a certain value in the positive and negative direction determines the change in the stiffness of suspension.

6

3 Numerical Experiment of a Spatial Motion Model of an Automobile

Mechanomathematical modeling of vehicle's motion with front-wheel drive, in the presence of a modern active safety system, active suspension, is associated with analysis of the change of angle around its own longitudinal and transverse axis of the car.

Technical data of an automobile are: mass $m = 1180 \text{ kg}$; length $a = 4,31 \text{ m}$; width $b = 1,74 \text{ m}$; longitudinal base $b = 2,65 \text{ m}$.

Initial linear and angular velocity of the car are as follows:

$$\begin{aligned} V_x &= 100 \text{ km/h}; V_y = 0 \text{ km/h}; V_z = 0 \text{ km/h} \\ \dot{\psi} &= 0 \text{ s}^{-1}; \dot{\theta} = 0 \text{ s}^{-1}; \dot{\varphi} = 0 \text{ s}^{-1} \end{aligned} \quad (19)$$

Elastic constants of springs without active and with active suspension are as follows:

$$\begin{aligned} c_i &= [20000 \quad 20000 \quad 18000 \quad 18000] \text{ [N/cm]} \\ c_{i1} &= [100000 \quad 100000 \quad 100000 \quad 100000] \text{ [N/cm]} \end{aligned} \quad (20)$$

Damping factor without active and with active suspension is as follows:

$$\begin{aligned} \beta_i &= [5246 \quad 5246 \quad 4208 \quad 4208] \text{ [N} \cdot \text{s/cm]} \\ \beta_{i1} &= [11731 \quad 11731 \quad 9919 \quad 9919] \text{ [N} \cdot \text{s/cm]} \end{aligned} \quad (21)$$

Initial linear coordinates of the center of mass and angles of rotation:

$$\begin{aligned} x_c &= 0 \text{ m}; y_c = -1,5 \text{ m}; z_c = 0,55 \text{ m} \\ \psi &= 0^\circ; \theta = 0^\circ; \varphi = 0^\circ \end{aligned} \quad (22)$$

3.1 Numerical Experiment of Vehicle's Motion without the Presence of an Active System in Suspension

When active suspension system is not activated, the following graphical dependencies are present (Figs. 3 and 4):

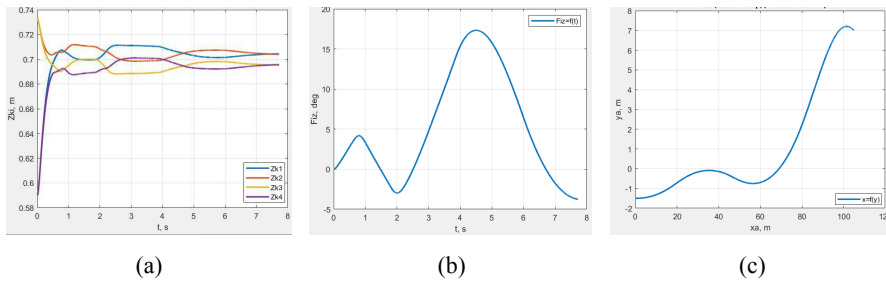


Fig. 3. (a) Coordinates of suspension points, (b) Changes in the angle around the Oz axis and (b) Trajectory of center of mass.

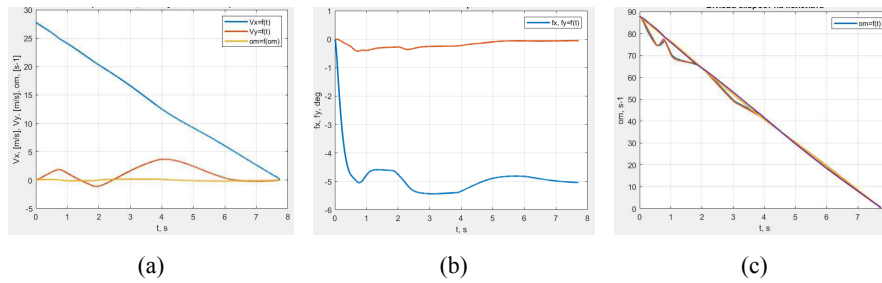


Fig. 4. (a) Center of mass velocity and angular velocity, (b) Changes in angle ϕ_x , and ϕ_y , and (b) Angular velocity of the wheels.

3.2 Numerical Experiment of Vehicle's Motion with the Presence of an Active System in Suspension

When active suspension system is activated, the following graphic dependencies are present (Figs. 5 and 6).

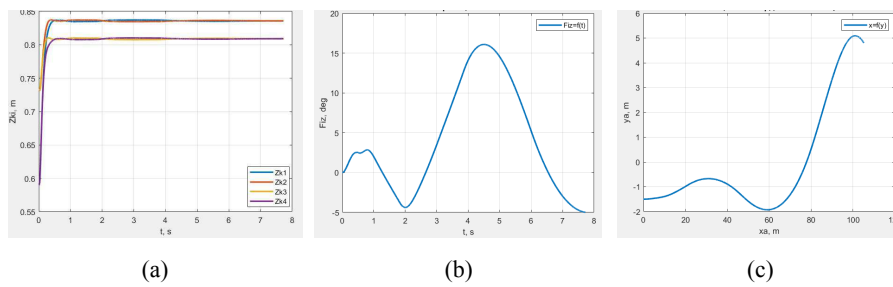


Fig. 5. (a) Coordinates of suspension points, (b) Changes in the angle around the Oz axis and (b) Trajectory of center of mass.

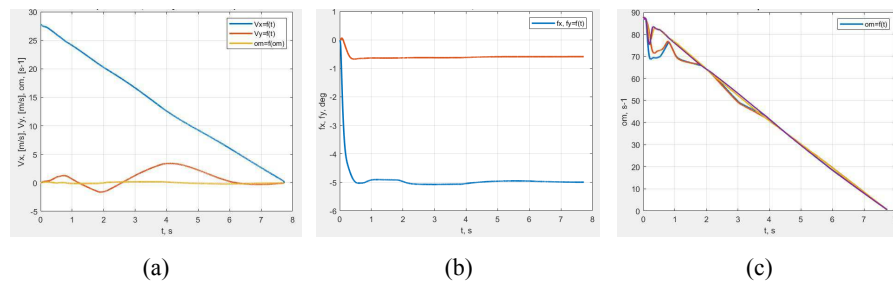


Fig. 6. (a) Center of mass velocity and angular velocity, (b) Changes in angle ϕ_x , and ϕ_y , and (b) Angular velocity of the wheels.

3.3 Comparative Analysis of Motion Trajectories and Critical Speed of an Automobile in a Turn. Critical Speed of a Vehicle's Curve

Examination of critical speed of an automobile is based on reduced tire-road friction coefficient of 0.7. The vehicle in motion is in successive curves without any inclination on the roadway (Fig. 7).



Fig. 7. Graphical measurement of the turning radius.

The radii of the turn with respect to the trajectory of the center of mass are obtained according to the dependence:

$$R_1 = \frac{a^2}{8.h} = \frac{40^2}{8.2,0} = 100 \text{ m} \quad (23)$$

$$R_2 = \frac{a^2}{8.h} = \frac{40^2}{8.0,82} = 244 \text{ m} \quad (24)$$

4 Conclusion

Maintaining vehicle's stability is achieved by reducing the influence of centrifugal inertial forces in the car body. Control and evaluation of the position of the vehicle body is by observing z-axis suspension of the body on each wheel and the slope angle of its own coordinate system relative to the invariably connected to the center of mass coordinate system parallel to the fixed coordinate system. The use of active suspension improves vehicle safety and increases reliability to prevent loss of lateral stability, but reduces ride comfort due to hardening suspension elasticity.

Acknowledgements. The authors would like to thank the Research and Development Sector at the Technical University of Sofia for the financial support.

References

1. Daily, J., Shigemura, N., Daily, J.: Fundamentals of Traffic Crash Reconstruction. Institute of Police Technology and Management, Florida (2006).
2. Schmidt, B.F., Haight, W.R., Szabo, T.J., Welcher, J.B: System-based energy and momentum analysis of collisions. SAE Trans. 107(6), 120–132 (1998).

3. Sharma, D., Stern, S., Brophy, J.: An overview of NHTSA's crash reconstruction software WinSMASH. In: Proceedings of the 20th International Technical Conference on the Enhanced Safety of Vehicles, ESV 2007, pp. 1–13 (2007).
4. Wach, W.: Analiza deformacji samochodu według standardu CRASH3. Część 2: Pomiar głębokości odkształcenia (Analysis of motor vehicle deformation according to the CRASH3 standard. Part 2: Measurement of deformation depth). Paragraf na Drodze 12 (2003).
5. Dechkova, S.: Creation of multi-mass models in the SolidWorks and Matlab environment for crash identification. *Mach. Mech.* 119, 28–32 (2018).
6. Karapetkov, S.: Auto Technical Expertise. Technical University of Sofia, Sofia (2005).
7. Karapetkov, S.: Investigation of Road Traffic Accident, Technical Commentary on the Lawyer. Technical University of Sofia, Sofia (2010).
8. Karapetkov, S., Uzunov, H.: Dynamics of Transverse Resistance of a Car. Didada Consult, Sofia (2016).
9. Karapetkov, S., Dimitrov, L., Uzunov, H., Dechkova, S.: Identifying vehicle and collision impact by applying the principle of conservation of mechanical energy. *Transp. Telecommun.* 20(3), 191–204 (2019).
10. Karapetkov, S., Dimitrov, L., Uzunov, H., Dechkova, S.: Examination of vehicle impact against stationary roadside objects. *IOP Conf. Ser.: Mater. Sci. Eng.* 659, 012063-1–012063-13 (2019).
11. Jiang, T., Grzebieta, R. H., Rehnitz, G., Richardson, S., Zhao, X. L.: Review of car frontal stiffness equations for estimating vehicle impact velocities. In: Proceedings of the 18th International Technical Conference on the Enhanced Safety of Vehicles Conference, ESV 2003, pp. 1–11. Nagoya (2003).
12. Niehoff, P., Gabler, H.C.: The accuracy of WinSMASH delta-V estimates: The influence of vehicle type, stiffness, and impact mode. *Annu. Proc. Assoc. Adv. Automot. Med.* 50, 73–89 (2006).
13. Owsiański, R.: Szacowanie energii deformacji nadwozi kompaktowych samochodów osobowych (Estimation of the bodywork deformation energy of compact passenger cars). Paragraf na Drodze 4 (2007).
14. Stronge, W.: *Impact Mechanics*. Cambridge University Press, Cambridge (2000).